

Detection of preinvasive cancer cells

Early-warning changes in precancerous epithelial cells can now be spotted *in situ*.

More than 85% of all cancers originate in the epithelium that lines the internal surfaces of organs throughout the body. Although these are readily treatable provided they are diagnosed in one of the preinvasive stages¹, early lesions are often almost impossible to detect. Here we present a new optical-probe technique based on light-scattering spectroscopy that is able to detect precancerous and early cancerous changes in cell-rich epithelia.

Before they become invasive, at stages known as dysplasia and carcinoma *in situ*, early cancer cells alter the epithelial-cell architecture. In particular, the nuclei become enlarged, crowded and hyperchromatic (that is, they stain abnormally darkly with a contrast dye as a result of changes in their chromatin content). These warning signs have so far only been detectable by histological examination of biopsy specimens¹, but light-scattering spectroscopy now offers a biopsy-free means to measure the size distribution and chromatin content of epithelial-cell nuclei as an indicator of preinvasive neoplasia.

The diameter of non-dysplastic cell nuclei is typically 5–10 μm , whereas dysplastic nuclei can be as large as 20 μm across. Epithelial-cell nuclei can be modelled as transparent spheroids that are large in comparison to the wavelength of visible light (0.4–0.8 μm), and whose refractive index is higher than that of the surrounding cytoplasm because of their chromatin content. The spectrum of light backscattered by these particles contains a component that varies characteristically with wavelength², with this variation depending on particle size and refractive index.

For a collection of nuclei of different sizes, the light-scattering signal is a superposition of these variations, enabling the nuclear-size distribution and refractive index to be determined from the spectrum of light backscattered from the nuclei^{3,4}. Once the nuclear-size distribution and refractive index are known, quantitative measures of nuclear enlargement, crowding and hyperchromasia can be obtained.

However, only a small amount of the light incident on the tissue is backscattered by the epithelial-cell nuclei: the rest becomes randomized in direction by multiple scattering, producing a large background of diffusely scattered light that must be subtracted. We have used two tactics to accomplish this — mathematical modelling of the diffusive background³ and polarizing the incident light, which is depolarized by multiple scattering⁴ and enables the single backscattering

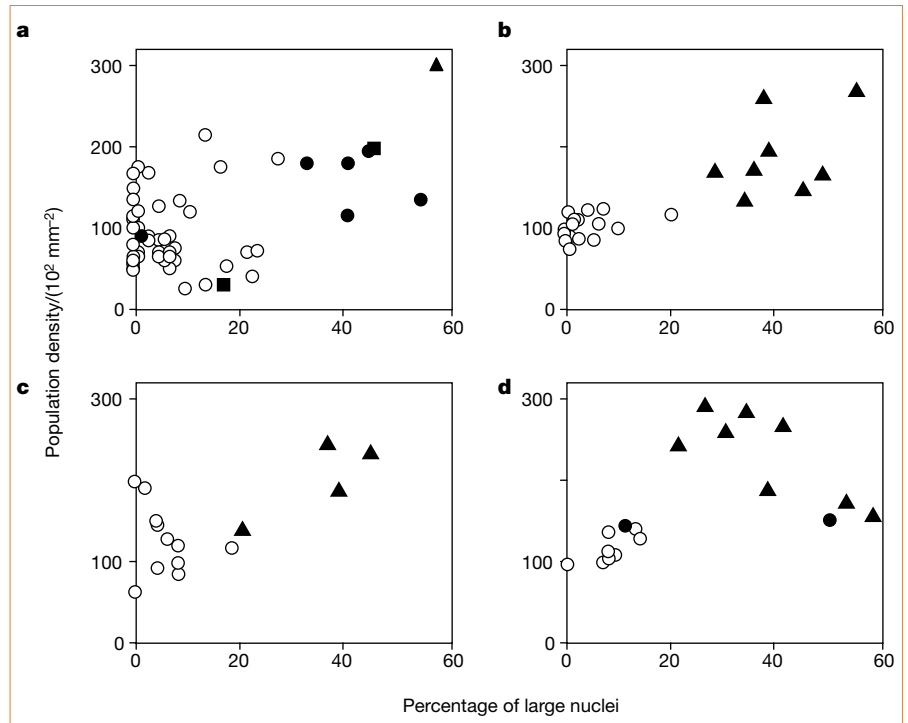


Figure 1 Classification of dysplasia and carcinoma *in situ* by light-scattering spectroscopy compared with diagnosis by histology for four types of epithelial tissue. The population density of nuclei, which determines nuclear crowding, is plotted against the percentage of enlarged nuclei. **a**, Barrett's oesophagus epithelium: circles, non-dysplastic Barrett's mucosa; squares, indefinite diagnosis for dysplasia; filled circles, low-grade dysplasia; triangle, high-grade dysplasia. **b**, Colon epithelium: circles, normal colonic mucosa; triangles, adenomatous polyp. **c**, Urinary bladder epithelium: circles, benign bladder mucosa; triangles, transitional cell carcinoma *in situ*. **d**, Oral cavity epithelium: circles, normal cells; filled circles, low-grade dysplasia; triangles, squamous-cell carcinoma *in situ*. Dysplasia in Barrett's oesophagus was studied during oesophagogastroduodenoscopy in 16 adults with a history of Barrett's oesophagus; colonic dysplasia was studied during colonoscopy in eight adults being screened for adenomatous colon polyps; carcinoma of the urinary bladder was investigated during cystoscopy in seven adults being screened for transitional-cell carcinoma or with a history of haematuria (blood in the urine). Testing for dysplasia and carcinoma in the oral cavity was done during routine oral examination in 5 adults suspected to have squamous-cell carcinoma. Informed consent from the patients was obtained in each case.

to be observed by subtracting the depolarized component of the backscattered light.

We have tested the potential of this technique *in vivo* to diagnose dysplasia and carcinoma *in situ* in four different human organs with three different types of epithelium: columnar epithelia of the colon and Barrett's oesophagus, transitional epithelium of the urinary bladder, and stratified squamous epithelium of the oral cavity. Our clinical investigations were all made during routine endoscopic screening or surveillance procedures, during which an optical-fibre probe delivered white light from a xenon arc lamp to the tissue surface and collected the returning light³.

The tip of the optical probe was brought gently into contact with the tissue under investigation. Immediately after measuring the backscattered light, a tissue biopsy sample was taken from the same site for histological examination. We analysed the spectrum of the reflected light from each

epithelium and determined the nuclear-size distribution of the epithelial cells.

We then used this nuclear-size distribution to obtain the percentage of nuclei larger than 10 μm across and the total number of nuclei per unit area (population density). As already noted, these parameters quantitatively characterize the degree of nuclear enlargement and crowding, respectively. Figure 1 shows these light-scattering spectroscopy parameters as binary plots to indicate the degree of correlation with histological diagnosis: in all four organs, there is a marked distinction between dysplastic and non-dysplastic epithelium. Both dysplasia and carcinoma *in situ* are associated with a higher percentage of enlarged nuclei and, on average, a higher population density, which can be used as the basis for spectroscopic diagnosis.

Our results show that light-scattering spectroscopy has the potential to detect epithelial precancerous lesions and

preinvasive cancers throughout the body. The advantage of this technique over conventional diagnostic procedures is that it can provide objective, quantitative results in real time without the need for tissue removal. Because of its potential application in screening for endoscopically invisible lesions, this technique should significantly improve the efficiency of cancer screening and surveillance.

V. Backman*, M. B. Wallace†, L. T. Perelman*, J. T. Arendt*, R. Gurjar*, M. G. Müller*, Q. Zhang*, G. Zonios*, E. Kline‡, T. McGillican§, S. Shapshay§, T. Valdez§, K. Badizadegan||, J. M. Crawford¶, M. Fitzmaurice#, S. Kabani§, H. S. Levin☆, M. Seiler**, R. R. Dasari*, I. Itzkan*, J. Van Dam†, M. S. Feld*

*Laser Biomedical Research Center, G. R. Harrison Spectroscopy Laboratory, Massachusetts Institute of Technology, Cambridge, Massachusetts 02139, USA
e-mail: msfeld@MIT.edu

†Division of Gastroenterology, Brigham and Women's Hospital, Boston, Massachusetts 02115, USA

‡Department of Urology, Cleveland Clinic Foundation, Cleveland, Ohio, 44106, USA

§New England Medical Center, Boston, Massachusetts 02132, USA

||Department of Pathology, Children's Hospital, Boston, Massachusetts 02115, USA

¶Department of Pathology, Yale University School of Medicine, New Haven, Connecticut 06520-8023, USA

#Department of Pathology, University Hospitals of Cleveland and Case Western Reserve University, Cleveland, Ohio 44106, USA

☆Department of Pathology, Cleveland Clinic Foundation, Cleveland, Ohio 44106, USA

**US Veteran Administration Hospital, West Roxbury, Massachusetts 02132, USA

1. Cotran, R. S., Robbins, S. L. & Kumar, V. *Robbins Pathological Basis of Disease* (Saunders, Philadelphia, 1994).
2. Van de Hulst, H. C. *Light Scattering by Small Particles* (Dover, New York, 1957).
3. Perelman, L. T. *et al. Phys. Rev. Lett.* **80**, 627–630 (1998).
4. Backman, V. *et al. IEEE J. Sel. Top. Quant.* **5**, 1019–1026 (1999).

sequence tags of preparasitic juveniles (J2s) of the potato-cyst nematode *Globodera rostochiensis*. One expressed sequence tag (*ge222*) encoded a partial open reading frame with similarity to bacterial and fungal pectate lyases (EC 4.2.2.2). A full-length complementary DNA sequence, which included the *ge222* tag, was subsequently obtained by the rapid amplification of cDNA ends by using messenger RNA from *G. rostochiensis* J2s as starting material².

The full-length cDNA contained a predicted open reading frame encoding a peptide sequence (PEL-1) of relative molecular mass 28K, with a signal sequence for secretion at its amino terminus. We expressed this coding region in *Pichia pastoris* to produce the active pectate lyase. We also found active pectate lyase in homogenates of *G. rostochiensis* J2. A digoxigenin-labelled DNA probe amplified from *pel-1* hybridized specifically to the subventral oesophageal gland cells, which also secrete cellulases³. These oesophageal gland cells are free of any symbiotic microorganisms³.

The PEL-1 sequence shows highest similarity (*E*-value of $5e^{-19}$ in BLAST-P⁴) with class III pectate lyases of bacterial and fungal origin (27–34% identity and 46–53% amino-acid similarity)⁴. Pectate lyases are divided into five classes, of which only class I (the pectate lyase superfamily) and class II (for example, periplasmic pectate lyase of *Erwinia carotovora*) have been characterized⁵; structural and functional information is sparse for class III pectate lyases.

Classification of PEL-1 as a class III pectate lyase markedly reduces the number of invariant amino-acid residues in this group (Fig. 1). Class III pectate lyases have four highly conserved regions and are characterized by the presence of several cysteine residues (eleven in PEL-1). On the basis of comparison of the PEL-1 sequence with other class III pectate lyases, only four conserved amino-acid residues with charged side chains (two aspartate residues at positions 130 and 199, and two lysine residues at positions 137 and 160) are present in the conserved regions. It is therefore likely that one or more of these invariant residues are involved in the catalytic machinery of PEL-1 and other class III members.

Symbiont-independent degradation of plant-cell walls by animals is now recognized as being possible. An endogenous cellulase gene was first isolated from cyst nematodes²; cellulases are also produced by termites⁶ and the redclaw crayfish (*Cherax quadricarinatus*)⁷. Our current finding demonstrates that, like bacteria and fungi, cyst nematodes are genetically equipped to secrete a mixture of depolymerizing cellulase and pectinase enzymes that allow the basic framework of plant cell walls to be dismantled.

Herman Popeijus*, Hein Overmars*, John Jones†, Vivian Blok†, Aska Goverse*,

Enzymology

Degradation of plant cell walls by a nematode

Interwoven networks of cellulose and pectin are the main components of plant cell walls¹, making them recalcitrant structures that can only be degraded by organisms producing a mix of synergistically acting enzymes. Animals were believed

to be unable to synthesize these enzymes, depending instead on symbiotic microbes to render plants into a food source. Here we describe a metazoan pectinase gene that encodes a pectate lyase for breaking down the pectin component of plant cell walls. To our knowledge, this is the first example of non-symbiotic degradation of pectin in plant cell walls by an animal.

We cloned the pectate lyase gene as part of a project analysing 1,000 expressed

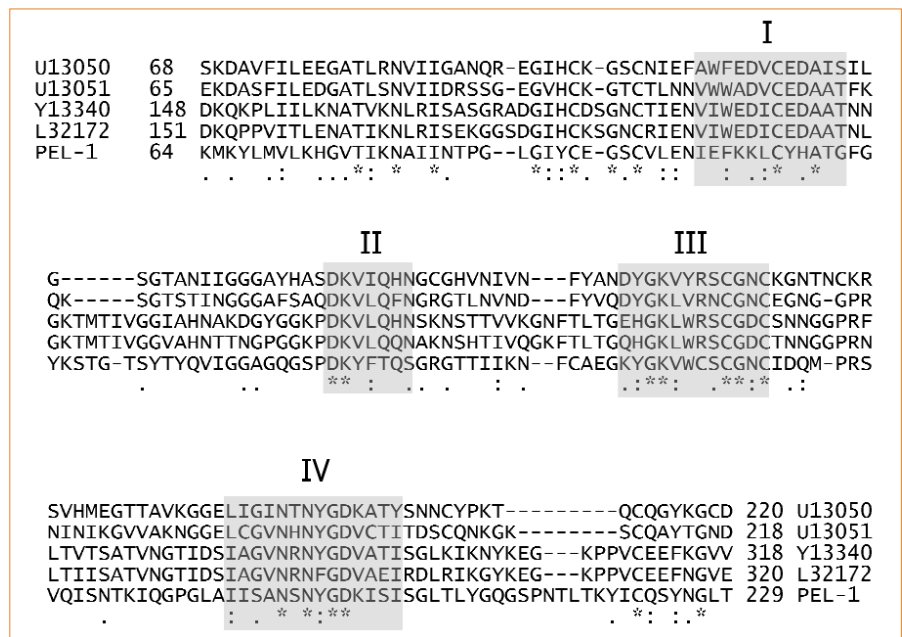


Figure 1 Predicted amino-acid sequence of *Globodera rostochiensis* PEL-1 (Genbank accession no. AF127915) aligned with bacterial (accession no. Y13340, *Erwinia chrysanthemi* Pel I, accession no. L32172, *E. carotovora* PelA) and fungal (accession no. U13050, *Nectria haematococca* Pel D, and accession no. U13051, *N. haematococca* Pel B) class III pectate lyases. Boxed shaded residues are conserved regions I to IV, as described for class III pectate lyase⁵. The alignment was made by using the program ClustalW and the BLOSUM62 substitution matrix. Asterisks, identical or conserved residues in all sequences in the alignment; colons, conserved substitutions; single dots, semiconserved substitutions⁸.